A MODEL FOR IMAGE SPLICING

Tian-Tsong Ng and Shih-Fu Chang

Department of Electrical Engineering, Columbia University, New York
{ttng,sfchang}@ee.columbia.edu

ABSTRACT

The ease of creating image forgery using image-splicing techniques will soon make our naïve trust on image authenticity a thing of the past. In prior work, we observed the capability of the bicoherence magnitude and phase features for image splicing detection. To bridge the gap between empirical observations and theoretical justifications, in this paper, an image-splicing model based on the idea of bipolar signal perturbation is proposed and studied. A theoretical analysis of the model leads to propositions and predictions consistent with the empirical observations.

1. INTRODUCTION

Image splicing, herein defined as a cut-and-paste of image regions from one image onto the same or another image without post-processing, is the basic operation for creating a digital photomontage, i.e., a paste-up of digital photographic regions.

Photomontage, with a root as old as the history of camera, is now a looming threat for our naïve trust on image authenticity. The advent of the modern digital technology has not only brought about the prevalent use of digital images in our daily activities but also the ease of creating image forgery using public accessible and user-friendly image processing tools such as Photoshop. Hence, the need for image authenticity assurance and detection of image forgery such as photomontage becomes increasingly acute as digital images take the role as news photographs, legal evidence and digital financial documents.

Active image authentication approaches include digital watermark and digital signature. However, when the prior knowledge of an image is unavailable, passive approaches become important. Human experts could analyze an image for any potential scene-level inconsistencies [1], such as a misplaced shadow, with special attentions given to minor details which forgers are likely to overlook. We recently experimented with the use of the bicoherence features for detecting image splicing and evaluated their effectiveness by classification experiments using Support Vector Machine based on a data set consisting of authentic and spliced image blocks [2, 3]. Without incorporating the improvement methods, the baseline bicoherence magnitude and phase features achieved on average 62% in authentication classification accuracy. This indicates the capability of the bicoherence features for image splicing detection. However, theoretical justification for the approach was missing. In our work, we consider an image as authentic as long as it is a direct output from an imaging device, even when the imaged object or scene is synthetic.

In this paper, we propose a model for image splicing which provides an insight into our previous empirical findings. The model is intuitively meaningful and predicts a phase bias at $\pm 90^o$, which is also observed in [3]. Examples of $\pm 90^o$ phase bias for spliced images are shown in Figure 1. In the next section, we look at related prior work on audio splicing. After a brief introduction to bicoherence, the proposed image-splicing model is outlined and a theoretical analysis for the response of the bicoherence magnitude and phase features to image splicing is performed based on the model. Finally, the theoretical findings are validated by empirical observations based on a data set.

2. PRIOR WORK

In [4], bicoherence magnitude and phase features are applied for detecting human speech splicing and the approach is justified with the following arguments:

1. Human speech signal is originally weak in higher order correlation, reflecting on the low value of the bicoherence magnitude feature.
2. A quadratic operation, by inducing a Quadratic Phase Coupling (QPC) phenomenon, increases the bicoherence feature values due to the quadratic harmonic relation and the 0^o phase bias. A general non-linear operation, when expressed by a Taylor expansion, has a partial sum of low-order terms resembling a quadratic operation.

However, the arguments could not justify the use of bicoherence features for image splicing detection:

1. Image signal may not be originally weak in higher order correlation as demonstrated in [5].
2. In [4], detection of a cascaded splicing and smoothing (using a Laplacian pyramid) operation on fractal signal and human speech signal is demonstrated. However, a splicing operation, if were to be considered a function, is potentially discontinuous and has no Taylor expansion. Thus, the aforementioned argument about QPC cannot be applied. Besides that, the effect on the bicoherence features due to splicing is still unknown.

3. BICOHERENCE FEATURES

Definition 1 (Bicoherence) *The bicoherence of a signal x(t) with its Fourier transform being X(ω) is given by [6]:*

$$b(\omega_1,\omega_2)=\frac{E[X(\omega_1)X(\omega_2)X^*(\omega_1+\omega_2)]}{\sqrt{E[\left|X(\omega_1)X(\omega_2)\right|^2]E[\left|X(\omega_1+\omega_2)\right|^2]}}=\left|b(\omega_1,\omega_2)\right|e^{j\Phi(b(\omega_1,\omega_2))}$$

Bicoherence is obtained by normalizing the bispectrum of the signal (numerator) with the Cauchy-Schwartz upper bound. Bispectrum refers to the Fourier transform of the third order

moment of a signal. We employed the bicoherence magnitude and phase features for image splicing in [2].

Definition 2 (Bicoherence Phase Histogram) *An N-bin bicoherence Phase histogram given by:*

$p(\Psi_n) = (1/M^2)\sum_{\Omega} 1(\Phi(b(\omega_1, \omega_2)) \in \phi)$, *1(·) = indicator function*

where

$\Omega=\{(\omega_1, \omega_2)|\ \omega_1=(2\pi m_1)/M,\ \omega_2=(2\pi m_2)Mm,\ m_1, m_2= 0,\ldots,.M-1\}$

$\Psi_n=\{\phi|(2n-1)\ \pi/(2N+1)\leq\phi< (2n+1)\ \pi\ /(2N+1)\}$, $n=-N,.. ,0,.. ,N$

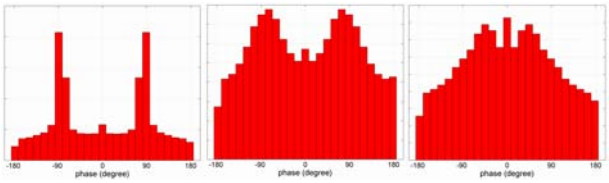

Figure 1 Typical examples of bicoherence phase histogram from spliced images: (Left) Strong ±90° phase bias (Middle) near ±90° phase bias (Right) non ±90° phase bias

Definition 3 (Bicoherence Magnitude Feature) *The magnitude feature is the mean of the magnitude of the bicoherence:*

$f_M =(1/M^2)\sum_{\Omega}|b(\omega_1, \omega_2)|$

Definition 4 (Bicoherence Phase Feature) *The phase feature which measures the non-uniformity or the bias of the bicoherence phase histogram:* $f_P=\Sigma_n p(\Psi_n)\log p(\Psi_n)$

Proposition 1 (Symmetry of Bicoherence Phase Histogram) *For a real-valued signal, the N-bin bicoherence phase histogram is symmetrical:* $p(\Psi_n) = p(\Psi_{-n})$ *for all n*

Proof The Fourier transform of a real-valued signal is conjugate symmetric, i.e., $X(\omega)= X^*(-\omega)$, hence, from Definition 1, its bicoherence is also conjugate symmetric, i.e., $b(\omega_1, \omega_2)= b^*(-\omega_1, -\omega_2)$. Therefore, its bicoherence phase histogram is symmetrical.

4. SPLICNG MODEL

Although image splicing is performed with 2-D regions, we detect the splicing through computing the bicoherence features of the vertical and horizontal 1-D slices of a spliced image [2]. In this paper, therefore, we propose a 1-D model for splicing, which is also applicable to the splicing of any 1-D signal. Here, we consider splicing a joining of signals without any post-processing of the spliced signal.

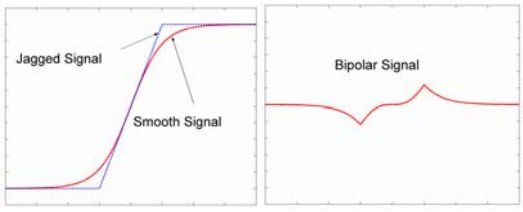

Figure 2 (Left) a jagged signal exhibits abrupt changes when compared to a smooth signal. (Right) the difference between the jagged and the smooth signals

A composite signal, due to the splicing of two signal segments, is very likely to introduce a discontinuity or an abrupt change at the splicing point. The lack of smoothness can be thought of a departure from a smooth signal due to a perturbation of a bipolar signal (Figure 2), which is similar to Haar high pass basis.

As almost every camera is equipped with an optical low pass filter and almost every scanner has a post-scanning low pass operation for avoiding aliasing effect which produces Moiré pattern, authentic images, being a direct output from image acquisition devices such as camera and scanner, could be modeled as a 'smooth' signal. With the idea of the authentic counterpart [2] (i.e., a possibly hypothetical but authentic image that resembles the spliced image in every respect except for those properties induced by splicing), we can model image splicing as a perturbation of the authentic counterpart with a bipolar signal.

Definition 5 (Bipolar signal) *A bipolar at location* x_o *with the antipodal delta separated by* Δ, *and with* k_1 *and* k_2 *being of opposite sign, i.e.,* $k_1 k_2<0$, *is represented as*

$d(x)=k_1\delta(x-x_o)+k_2\ \delta(x-x_o-\Delta)$, $\delta(\cdot)$ *being a delta function and its Fourier Transform is* $D(\omega) = k_1 e^{-jx_o\omega} + k_2 e^{-j(x_o+\Delta)\omega}$

4.1. Response of Bicoherence Phase Feature

As the phase of a bicoherence is equal to the phase of numerator of the expression in Definition 1, therefore, it suffices to examine the numerator as far as the response of the bicoherence phase feature is concerned.

Proposition 2 (Phase of Bipolar Signal Bicoherence) *Assuming* $k_1 = -k_2 = k$, *the phase of the bicoherence for a bipolar signal is concentrated at ±90°.*

Proof When $k_1 = -k_2 = k$, *the third-order moment of* $D(\omega)$:

$D(\omega_1)D(\omega_2)D^*(\omega_1+\omega_2)=2k^3j[\sin\Delta\omega_1+\sin\Delta\omega_2-\sin\Delta(\omega_1+\omega_2)]$ (1)

is an imaginary number. The expectation of an imaginary random number is still an imaginary number with a phase at ±90°.

It is interesting to observe that the phase bias at ±90° is not due to QPC which could in turn give rise to 0° phase bias. QPC is due to the existence of harmonics with the same frequency and phase relationship, e.g., when there exists harmonics at ω_1, ω_2 and $\omega_1+\omega_2$ for the Fourier transform of a signal $S(\omega)$, the phase of the harmonics are φ_1, φ_2 and $\varphi_1+\varphi_2$ respectively, hence, $phase[S(\omega_1)S(\omega_2)] = phase[S(\omega_1+\omega_2)]$. However, for the bipolar signal, the phase relationship is given by $phase[D(\omega_1)D(\omega_2)] = phase[D(\omega_1+\omega_2)] \pm \pi/2$.

On the other hand, when $k_1 = k$ *and* $k_2 = -k+\varepsilon<0$,

$$D(\omega_1)D(\omega_2)D^*(\omega_1+\omega_2) = \varepsilon(3k^2-3k\varepsilon+\varepsilon^2)+ k\varepsilon(\varepsilon-k)[\exp(j\Delta\omega_1)+ \exp(-j\Delta\omega_2)+ \exp(j\Delta(\omega_1+\omega_2)]+ 2k^2(k-\varepsilon)j[\sin\Delta\omega_1+\sin\Delta\omega_2-\sin\Delta(\omega_1+\omega_2)] \quad (2)$$

Therefore, if ε is small relative to k, in equation (2), the last term becomes dominant and the phase remains concentrated around ±90°. In other words, if the magnitudes of the opposite poles of the bipolar are approximately equal, the ±90° phase concentration occurs.

Before moving on to Proposition 3, please note that, in practice, bicoherence is computed by:

$$\hat{b}(\omega_1,\omega_2)=\frac{\frac{1}{k}\sum_k X_k(\omega_1)X_k(\omega_2)X_k^*(\omega_1+\omega_2)}{\sqrt{\left(\frac{1}{k}\sum_k\left|X_k(\omega_1)X_k(\omega_2)\right|^2\right)\left(\frac{1}{k}\sum_k\left|X_k(\omega_1+\omega_2)\right|^2\right)}}$$

where the expectation terms are estimated by the average terms with a *set of signal segments* from the target 1-D signal [2].

When a signal *s(x)*, is perturbed by a bipolar signal, *d(x)*, the resulting perturbed signal and its Fourier transform is given by:

$$s_p(x)=s(x)+d(x) \leftrightarrow S_p(\omega)=S(\omega)+D(\omega)$$

Proposition 3 (Response of Bicoherence Phase Feature) *Perturbation of a signal with a bipolar contributes to a phase bias at ±90°. The strength of the overall contribution is dependent on (1) the magnitude of the bipolar (2) the percentage of bipolar perturbed segments within the set of signal segments used for computing the bicoherence by averaging.*

Proof For simplicity, assume that $k_1 = -k_2 = k$ for the magnitude of the bipolar, the correlation of the Fourier transform of the perturbed signal is given by:

$$S_p(\omega_1)S_p(\omega_2)S_p^*(\omega_1+\omega_2) = S(\omega_1)S(\omega_2)S^*(\omega_1+\omega_2)+ \text{cross terms}+2k^3j[\sin\Delta\omega_1+\sin\Delta\omega_2-\sin\Delta(\omega_1+\omega_2)] \quad (3)$$

where

$$\text{cross terms} = kS(\omega_1)S^*(\omega_1+\omega_2)\exp(-jx_o\omega_2)[1-\exp(-j\Delta\omega_2)]+ kS(\omega_2)S^*(\omega_1+\omega_2)\exp(-jx_o\omega_1)[1-\exp(-j\Delta\omega_1)]+k^2S^*(\omega_1+\omega_2)\exp(-jx_o(\omega_1+\omega_2))[1-\exp(-j\Delta\omega_1)][1-\exp(-j\Delta\omega_2)]+ kS(\omega_1)S(\omega_2)\exp(jx_o(\omega_1+\omega_2))[1-\exp(j\Delta(\omega_1+\omega_2))]+ k^2S(\omega_1)\exp(jx_o\omega_1)[1-\exp(-j\Delta\omega_2)][1-\exp(j\Delta(\omega_1+\omega_2))]+ k^2S(\omega_2)\exp(jx_o\omega_2)[1-\exp(-j\Delta\omega_1)][1-\exp(j\Delta(\omega_1+\omega_2))]$$

We can see that the imaginary term due to bipolar perturbation contribute consistently at every (ω_1, ω_2) to the imaginary component of equation (3). The strength of the contribution depends on *k*. The same argument is applicable to the case when $k_1 = k$ and $k_2 = -k+\varepsilon<0$ with ε being small relative to *k,* but the strength of the contribution is lessened.

As numerator of bicoherence expression is estimated by an average of the third-order moment for the Fourier transform of a signal over a set of signal segments, the percentage of bipolar perturbed segment within the set affects the contribution to ±90° phase bias. In actual case, we estimate the bicoherence of a 1-D image slice of length 128 pixels with 3 overlapping segments of length 64 pixels [2, 3]. The overlap of segments ensures a larger extent of the perturbation effect, as a splicing point is likely to be captured by two adjacent segments with a probability of 0.5, assuming uniformly distributed splicing point.

4.2. Response of Bicoherence Magnitude Feature

When examining the response for the bicoherence magnitude feature, we need to consider the entire expression from Definition 1, including the normalization term.

Proposition 4 (Response of Bicoherence Magnitude Feature) *Perturbation of a signal with a bipolar signal contributes to an increase in the value of the bicoherence magnitude feature. The amount of the increase depends on (1) the magnitude of the bipolar relative to the mean of the magnitude of the original signal Fourier transform (2) the percentage of bipolar perturbed segments within the set of signal segments used for computing the bicoherence by averaging.*

Proof For simplicity, we analyze the perturbation with a bipolar having $k_1 = -k_2 = k$. Note that the sign of equation (1) at a particular (ω_1, ω_2) is determined by the separation (denoted by Δ) and the orientation (denoted by the sign of *k*) of the poles of a bipolar signal. With the following assumptions on the bipolar across the ensemble of signal used for estimating bicoherence, $D(\omega_1)D(\omega_2)$ would be equal to $D(\omega_1+\omega_2)$ within a constant for a particular (ω_1, ω_2).

- The orientation of the bipolars is the same. (This assumption is reasonable as the same bipolar can be captured by two different but overlapping windows.)
- The pole separation for the bipolar is the same (This assumption is also valid because the bipolar introduced by splicing is compact at the splicing interface)
- The magnitude of bipolar is the same.

When $D(\omega_1)D(\omega_2) = c(\omega_1,\omega_2)D(\omega_1+\omega_2)$ with $c(\omega_1,\omega_2)$ being a constant for a particular (ω_1,ω_2), the magnitude of the bicoherence is 1 at every frequencies (ω_1, ω_2), as, in this case, the numerator of Definition 1 attains the Cauchy-Schwartz inequality upper bound. When a signal *s(x)* with Fourier transform *S(ω)* is perturbed by a bipolar, the magnitude of the bicoherence is given by:

$$|b(\omega_1,\omega_2)|=\frac{\left|E[k^3[\frac{S(\omega_1)}{k}+G(\omega_1)]\cdot[\frac{S(\omega_2)}{k}+G(\omega_2)]\cdot[\frac{S^*(\omega_1+\omega_2)}{k}+G^*(\omega_1+\omega_2)]]\right|}{\sqrt{E[k^4\left|[\frac{S(\omega_1)}{k}+G(\omega_1)]\cdot[\frac{S(\omega_2)}{k}+G(\omega_2)]\right|^2]E[k^2\left|\frac{S(\omega_1+\omega_2)}{k}+G^*(\omega_1+\omega_2)\right|^2]}} \quad (4)$$

where $G(\omega)=\exp(-jx_o\omega)\,[1-\exp(-j\Delta\omega)]$

From Markov inequality, the term $|S(\omega)/k|$ in equation (4) is upper-bounded in probability by $P(|S(\omega)/k| \geq \varepsilon) \leq E[S(\omega)]/(k\varepsilon)$, for any all $\varepsilon>0$. Hence, for an energy signal, i.e., signal with finite energy such as normal image signal, $\lim_{k\to\infty} P(|S(\omega)/k| \geq \varepsilon) = 0$, for $E[S(\omega)]$ being finite. As a result, the magnitude of bicoherence $|b(\omega_1, \omega_2)|$ in equation (4) satisfies:

$$\lim_{k\to\infty} P\left(\left|b(\omega_1,\omega_2)\right|-\frac{|E[D(\omega_1)D(\omega_2)D^*(\omega_1+\omega_2)]|}{\sqrt{E[|D(\omega_1)D(\omega_2)]|^2]E[|D^*(\omega_1+\omega_2)|^2]}}\right|\geq\varepsilon\Bigg)=0$$

With the above assumptions: $\lim_{k\to\infty}P(|\,|b(\omega_1, \omega_2)| - 1\,| \geq \varepsilon) = 0$

Therefore, the more frequency triplets with a small $E[S(\omega)]$ relatively to *k*, the greater the contribution of the bipolar perturbation to an increase in the bicoherence magnitude feature.

Similar to the bicoherence phase feature, the extent of bipolar perturbation in the ensemble of signal is another factor affecting the contribution of bipolar perturbation to an increase in bicoherence magnitude feature.

5. VALIDATION BY EXPERIMENT

5.1. Data Set Description

Our data set (available at [7]) is collected with sample diversity in mind. It has 933 authentic and 912 spliced image blocks of size 128 x 128 pixels. The image blocks are extracted from images in CalPhotos image set [8]. As the images are contributions from photographers, we assume that they can be considered authentic i.e., not digital photomontages.

The authentic category consists of image blocks of an entirely homogenous textured or smooth region and those having an object boundary separating two textured regions, two smooth regions, or a combination of a textured region and a smooth

region. The location and the orientation of the boundaries are random. The spliced category has the same subcategories as the authentic one. For the spliced subcategories with object boundaries, image blocks are obtained from images with spliced objects; hence, the splicing region interface coincides with an arbitrary-shape object boundary. Whereas for the spliced subcategories with an entirely homogenous texture or smooth region, image blocks are obtained from those in the corresponding authentic subcategories by copying a vertical or a horizontal strip of 20 pixels wide from one location to another location within a same image.

5.2. Validation for Bicoherence Features

With the above-mentioned data set, by examining the difference of the mean of the phase histogram (Definition 2) for the authentic and spliced categories of our data set (Figure 3), a clear statistical difference of phase bias for the two categories at $\pm 90^o$ is observed. This observation supports the theoretical prediction of the $\pm 90^o$ phase bias (Proposition 2) based on the proposed image-splicing model. Note that, from Proposition 1, it suffices to study the positive half of the bicoherence phase histogram (i.e. from 0^o to 180^o). Figure 1 shows two examples of $\pm 90^o$ phase bias from spliced images.

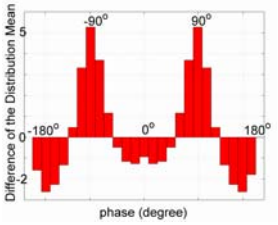

Figure 3 The mean of the authentic phase histogram minus the mean of the spliced phase histogram

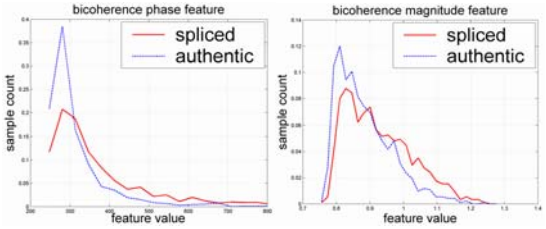

Figure 4 The histogram of the bicoherence features: (Left) phase feature (Right) magnitude feature

In addition, the histogram for bicoherence magnitude and phase features (Figure 4) for the spliced category is observed to have a larger mean and a heavier tail compared to that of the authentic category. This validates the Proposition 3 and 4.

5.2. 90^o Phase Bias as Prediction Feature

To evaluate the performance 90^o phase bias as a feature for image splicing detection, we performed the same classification experiments as in [2] by replacing the negative phase entropy with the 90^o phase bias, which is measured by the value of the bicoherence phase histogram at 90^o. The results of detection accuracy over the same data set are comparable at about 70%. This indicates that the negative phase entropy, despite being a general measure of phase bias, has already captured the specific effect of 90^o phase bias. The fact that the feature using the specific 90^o phase bias fails to achieve noticeable improvement indicates the weakness of the phase bias effect, which is linked to the high estimation variance that commonly plagues the estimation of higher order statistics such as bicoherence.

6. CONCLUSIONS

We have proposed an image-splicing model based on the idea of bipolar perturbation of an authentic signal and performed a theoretical analysis for the response of the bicoherence magnitude and phase features to splicing based on the proposed model. The analysis leads to the final propositions that image splicing increases the value of the bicoherence magnitude and phase features and a prediction of $\pm 90^o$ phase bias, which both are shown to be consistent with the empirical observations based on our data set.

The proposed model has founded the use of bicoherence magnitude and phase features for image splicing detection on a sound theoretical ground. Bicoherence could become more powerful for image splicing detection if such capability of bicoherence can be further isolated from the interference of other non-splicing factors, as demonstrated in [2]. We will study the image-splicing model further in hope that other useful image splicing detection features of bicoherence in particular or higher order statistics in general could be identified.

7. ACKNOWLEDGEMENTS

Our heartfelt gratitudes to Prof. Mao-Pei Tsui and Prof. Aileen Tsui for the beneficial discussions and to Singapore A*STAR for sponsoring the first author.

8. REFERENCES

[1] W. J. Mitchell, "When Is Seeing Believing?", *Scientific American*, pp. 44-49, February 1994.

[2] T.-T. Ng, S.-F. Chang and Q. Sun, "Blind Detection of Photomontage Using Higher Order Statistics", *IEEE ISCAS,* to appear, May 2004.

[3] T.-T. Ng and S.-F. Chang, "Blind Image Splicing and Photomontage Detection Using Higher Order Statistics", *ADVENT Technical Report*, #201-2004-1, Columbia University, http://www.ee.columbia.edu/dvmm/, Jan 2004.

[4] H. Farid, "Detecting Digital Forgeries Using Bispectral Analysis", *Technical Report*, AIM-1657, MIT AI Memo, 1999.

[5] Krieger, G., Zetzsche, C. and Barth, E., "Higher-order statistics of natural images and their exploitation by operators selective to intrinsic dimensionality", *Proc. of IEEE Signal Processing Workshop on HOS*, pp. 147-151, 21-23 July 1997.

[6] Y. C. Kim and E. J. Powers, "Digital Bispectral Analysis and its Applications to Nonlinear Wave Interactions", *IEEE Trans. on Plasma Science,* vol. PS-7, No.2, pp. 120-131, June 1979.

[8] A data set of authentic and spliced image blocks, DVMM, Columbia Univ., http://www.ee.columbia.edu/dvmm/researchProjects/AuthenticationWatermarking/BlindImageVideoForensic/

[7] CalPhotos: A database of photos of plants, animals, habitats and other natural history subjects. Digital Library Project, University of California, Berkeley.